ChemComm

Crystallographic and spectroscopic characterization of a mixed actinide-lanthanide carbide cluster stabilized inside an Ih(7)-C80 fullerene cage

Journal:	*ChemComm*
Manuscript ID	CC-COM-01-2020-000133.R1
Article Type:	Communication

COMMUNICATION

Crystallographic and spectroscopic characterization of a mixed actinide-lanthanide carbide cluster stabilized inside an I_h(7)-C_{80} fullerene cage

Received 00th January 20xx,
Accepted 00th January 20xx

DOI: 10.1039/x0xx00000x

Xiaomeng Li[a]†, Yang-Rong Yao[b]†, Wei Yang[a], Jiaxin Zhuang[a], Luis Echegoyen[b], Ning Chen[a]*

A mixed actinide-lanthanide cluster fullerene, $Sc_2UC@I_h(7)$-C_{80}, was isolated and fully characterized. For the first time, the single crystal X-ray crystallographic analysis confirms a novel actinide-lanthanide cluster Sc_2UC stabilized inside an $I_h(7)$-C_{80} cage. Moreover, the U=C double bond distance is 2.01 Å, the shortest U=C bond confirmed by crystallography so far.

Endohedral cluster fullerenes have been extensively studied since the first discovery of $Sc_3N@I_h(7)$-C_{80} in 1999 by Dorn and co-workers.[1] Since then, variable lanthanide based metallic clusters, which otherwise are not stable independently, were stabilized by the encapsulation of fullerene cages.[2,3] This unique stabilization effect of fullerene cages provided an efficient method to trap and characterize thermodynamically unstable metallic clusters in a molecular structure. Most of the metallic cluster fullerenes reported so far are based on lanthanides. Actinide cluster fullerenes, which might stabilize novel actinide clusters and bonding motifs, remained unexplored for a long time.[4-10] Recently, we reported the synthesis of $U_2C@I_h(7)$-C_{80}, a major and interesting breakthrough in the field.[11] The unprecedented di-uranium carbide cluster contains two unsupported axial U=C double-bonds, with unexpectedly short uranium–carbon distances (2.03 Å). The successful synthesis of $U_2C@I_h(7)$-C_{80} and its unique bonding motif motivate us to further explore these novel actinide cluster fullerenes. Very recently, a mass signal at m/z 1300, observed in the fullerene soot mixture, was identified as the signal of $Sc_2UC@C_{80}$, the first mixed actinide-lanthanide cluster fullerene. A separation protocol was developed to isolate this compound and computational studies were employed to predict this fascinating structure.[12] However, its molecular structure has never been verified by experimental characterization, mainly due to the difficulty of the synthesis and isolation on macroscopic scale. Actinide chemists have devoted considerable efforts to synthesize uranyl-lanthanide heterometallic complexes due to their unique magnetic and luminescence properties generated by the synergistic effect of the two kinds of elements. However, reports of this type of compounds are still fairly rare, and most of those reported so far are in aggregation state such as 2D polymers or cage clusters.[13-16] To the best of our knowledge, $Sc_2UC@C_{80}$ is the first molecular compound that contains a mixed actinide-lanthanide cluster. Thus, crystallographic verification and characterization of this novel molecule is of significant importance for both fullerene and actinide chemistry. Herein, we report the crystallographic and spectroscopic characterization of $Sc_2UC@I_h(7)$-C_{80}. The crystallographic characterization unambiguously confirms the presence of Sc_2UC, a novel heterometallic 4f-5f carbide cluster, stabilized inside an $I_h(7)$-C_{80} cage.

The uranium-based endohedral fullerenes were synthesized by a modified Krätschmer-Huffman DC arc-discharge method[17] with a mixture of U_3O_8/Sc_2O_3/C powder (molar ratio of U/Sc/C = 1:2:30) under a He atmosphere of 200 Torr and 1 Torr NH_3. The collected raw soot was extracted by carbon disulfide (CS_2) for 24 h. After a four-stage high-performance liquid chromatography (HPLC) separation procedure (see Figure S1), the purified $Sc_2UC@C_{80}$ was obtained. The purity of $Sc_2UC@C_{80}$ was confirmed by the observation of a single peak by HPLC and as a sole peak at 1299.966 m/z by MALDI-TOF mass spectrometry, and the observed isotopic distribution agrees well with the theoretical calculation (see Figure S2).

Single crystal X-ray diffraction analysis was utilized for the structural determination of $Sc_2UC@I_h(7)$-C_{80}. Black blocks of $Sc_2UC@I_h(7)$-C_{80}·[Ni^{II}-OEP] (OEP = 2, 3, 7, 8, 12, 13, 17, 18-octaethylporphyrin dianion) were obtained by slow diffusion of a benzene solution of Ni^{II}-OEP into a CS_2 solution of $Sc_2UC@C_{80}$.

[a] *Laboratory of Advanced Optoelectronic Materials, College of Chemistry, Chemical Engineering and Materials Science, Soochow University. Suzhou, Jiangsu, 215123 (P. R. China).*
[b] *Department of Chemistry, University of Texas at El Paso. 500 W University Avenue, El Paso, Texas 79968 (United States)*
† These authors contributed equally to this work.
Electronic Supplementary Information (ESI) available: CCDC 1965581. For more experimental details See DOI: 10.1039/x0xx00000x

The refined crystal structure is shown in Figure 1a. The molecular structure was solved and refined in the *C*2/*c* (No. 15) space group. The host-guest interaction between $Sc_2UC@I_h(7)$-C_{80} and Ni^{II}-OEP is evident by the shortest Ni-to-cage-carbon distance of 2.87 Å, which is very close to those observed in the recently reported $U_2@I_h(7)$-C_{80}·[Ni^{II}-OEP] and $U_2C@I_h(7)$-C_{80}·[Ni^{II}-OEP] and to most EMF·[Ni^{II}-(OEP)] complexes.[11,18] The fullerene cage is ordered and can be unambiguously assigned to $I_h(7)$-C_{80}. The encapsulated cluster can be assigned to a mixed Sc_2UC cluster though it is slightly disordered. To the best of our knowledge, this is the first crystallographic observation of a mixed actinide-lanthanide metallic cluster. The tri-metallic carbide cluster inside the cage has a triangular shape, a rare configuration for endohedral carbide clusters, but resembles that of the recently reported $Ln_2TiC@I_h(7)$-C_{80} (Ln = Sc, Lu, Tb).[19-21] Crystallographic analysis suggests that the Sc_2UC cluster is motionally restricted. The central carbon is fully ordered, and interestingly, the metals exhibit four orientations, one major and three minor sites with occupancies of 0.588(2), 0.1419(15), 0.1102(14) and 0.0368(12), which are unexpectedly restricted to a narrow area (see Figure S3 and Table S1). More surprisingly, the minor uranium sites are located nearby the two Sc-favored sites instead of to the major uranium site. To fit the distribution of each minor uranium site, the rest of the corresponding Sc sites reside at the other two vertices of a triangle (Figure 1c). The crystallographic results suggest that rather than rotating around the cage, the hindered Sc_2UC cluster prefers to hop inside the cage. This motion is quite unique because in general, for mixed cluster fullerenes like $Sc_xV_{3-x}C@I_h(7)$-C_{80} (x = 1, 2), $LaSc_2N$-$@I_h(7)$-C_{80}, $LaSc_2N@C_s$(hept)-C_{80} and $Sc_2TiC@I_h(7)$-C_{80}, the disordered sites of each metal atom are confined in the vicinity of the major sites.[21-24] Nevertheless, similar cluster hopping phenomena have been observed in the recent studies of $TiLu_2C@I_h(7)$-C_{80} and $TiTb_2C@I_h(7)$-C_{80}, in which the Ti atom also has an oxidation state of +4 and forms a double bond with the central carbon.[19,20]

Figure 1b shows that in the major cluster orientation (occupancy of 0.588(2)), the metal-to-carbon distances are 2.053(6) Å, 2.060(6) Å and 2.011(5) Å for Sc1-C81, Sc2-C81 and U1-C81 bonds, respectively. The two Sc-C81 bond lengths are very close to that observed in $Sc_2TiC@I_h(7)$-C_{80}.[21] Notably, the U1-C81 bond length is even slightly shorter than the U=C double bond length in $U_2C@I_h(7)$-C_{80} (2.033 Å), which was the shortest U-C bond reported before the present case.[11] This U-C bond length proves that, similar to the case of $U_2C@I_h(7)$-C_{80}, the U-C bond in the Sc_2UC cluster is also a rare example of standard axial U=C double bond and it is the shortest U-C bond discovered in the U-containing molecules characterized by crystallography so far. The configuration of the Sc_2UC cluster can be described as two Sc-C single bonds and one U=C double bond radiated from the central C atom, which is similar to the previously reported $(Sc^{3+})_2Ti^{4+}C$ cluster. Our recent study shows that the two U atoms in $U_2C@I_h(7)$-C_{80} have a formal oxidation state of +5 and form two U=C double bonds with the central carbon atom.[11] The present result suggests that, when one U atom is replaced by two Sc atoms, the oxidation state of the U atom changes from +5 in U_2C cluster to +4 in Sc_2UC within the same cage of $I_h(7)$-C_{80}, which is in good agreement with recent theoretical prediction.[12,25] This observation highlights the remarkable flexibility of oxidation state of U inside fullerene cages. We recently reported for $U@C_{2n}$ (n=37,41) that the oxidation state of U can be dictated by the isomeric structure of the fullerene cages, changing from +4 to +3.[26,27] Here we observed that, in the endohedral cluster fullerenes, U can alter its oxidation state from +5 to +4, depending on the composition of the cluster, likely to facilitate a 6-electron cluster-to-cage charge transfer, which is essential to the stabilization of the $I_h(7)$-C_{80} cage. In fact, different from relatively stable oxidation states for the lanthanides, variable oxidation states are typical for actinides. The continuing study of actinide cluster fullerenes will very likely discover unexpected actinide clusters and bonding motifs, which have not been observed in conventional actinide chemistry or cluster fullerene studies.

The sum of metal-carbon-metal bond angles around C81 is about 359.9°, showing a highly planar structure. The U1 atom is located over a hexagon ring with U-C distances ranging from 2.493(6) Å to 2.535(6) Å, while the Sc1 and Sc2 atoms are individually situated over a 5:6 ring junction with Sc-C distances of 2.209(6) Å for Sc1-C56, 2.206(6) Å for Sc1-C55, 2.226(7) Å for Sc2-C78 and 2.198(6) Å for Sc2-C79, respectively. Consquently, the position of the central carbon of the Sc_2UC cluster is slightly away from the center of $I_h(7)$-C_{80} cage by about 0.19 Å. It is worth noting that the cluster-to-cage interactions of $Sc_2UC@I_h(7)$-C_{80} are quite different from that of $Sc_2TiC@I_h(7)$-C_{80}, in which either metal atom is close to a 6:6:5 junction,[21] and that of the $TiLu_2C@I_h(7)$-C_{80}, in which the Ti atom is adjacent to a 5:6 ring junction and the two Lu atoms are located near the center of hexagon.[19]

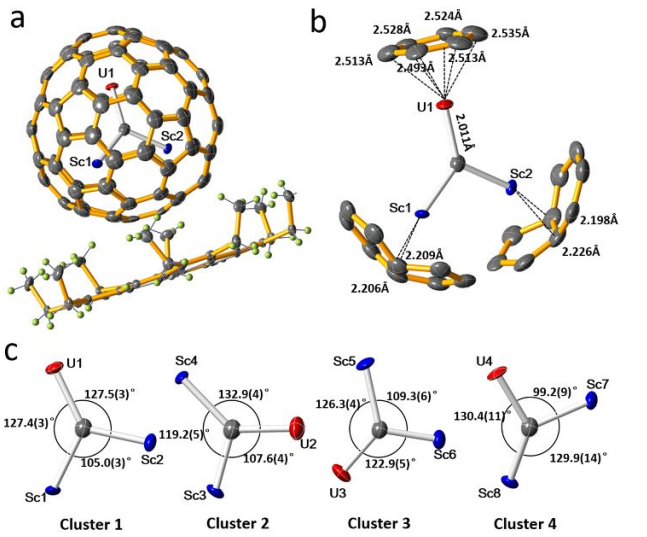

Figure 1. (a) The ORTEP drawing of $Sc_2UC@I_h(7)$-C_{80}·[Ni^{II}(OEP)] with 50% thermal ellipsoids. Only the Sc_2UC cluster in major orientation is shown, and the solvent molecules and minor atomic sites are omitted. (b) View of the relationship between the major Sc_2UC cluster and the closest cage portion. (c) Four orientations refined as occupancies of 0.588(2), 0.1419(15), 0.1102(14) and 0.0368(12) (corresponding to clusters 1-4, respectively) viewed from the same direction.

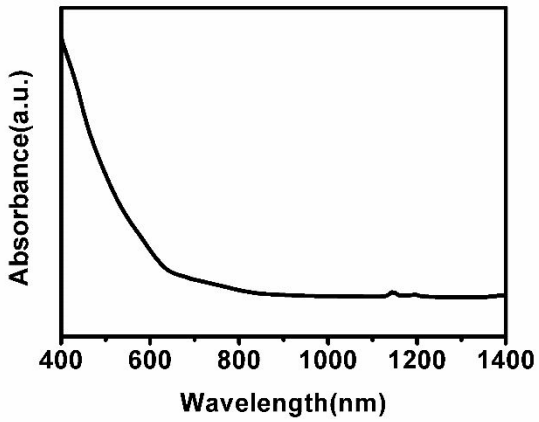

Figure 2. UV–vis–NIR absorption spectrum of $Sc_2UC@I_h(7)$-C_{80} in CS_2 solution.

The purified sample of $Sc_2UC@I_h(7)$-C_{80} dissolved in carbon disulphide (CS_2) was characterized by UV–vis–NIR absorption spectroscopy, as shown in Figure 2. The UV–vis–NIR absorption spectrum of $Sc_2UC@I_h(7)$-C_{80} is rather featureless except for a subtle deviation of the slope of the curve at 645 nm, with the absorption onset measured at about 950 nm and the optical band gap of 1.31 eV. The result coincides with those of the many EMFs with $I_h(7)$-C_{80} symmetry.[1,11,18]

Low-energy Raman emission and Fourier transform infrared absorption (FTIR) spectroscopy were utilized to further investigate the molecular vibrational features of $Sc_2UC@I_h(7)$-C_{80}, as shown in Figure 3 and 4. The Raman spectrum of $Sc_2UC@I_h(7)$-C_{80} can be roughly divided into two parts. Between 220 and 600 cm^{-1} are the vibrational modes of the carbon cage, which show significant similarity to those of previously reported EMFs with $I_h(7)$-C_{80} cage, such as $La_2@I_h(7)$-C_{80}, $U_2@I_h(7)$-C_{80} and $U_2C@I_h(7)$-C_{80}.[11,18,28] In the 100 to 220 cm^{-1} range, two prominent peaks at 146 cm^{-1} and 200 cm^{-1} can be observed. The two peaks could be rationally assigned to the split metal-cage stretching mode of the Sc_2UC cluster, a phenomenon frequently detected for EMFs with mixed clusters, such as $Gd_xSc_{3-x}N@C_{80}$(x = 1, 2).[29] In the IR absorption spectrum, the characteristic absorption bands in the high-wavenumber range from 1100 to

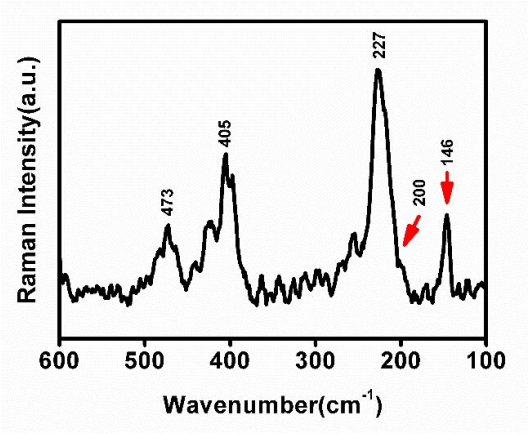

Figure 3. Low-energy Raman spectrum of $Sc_2UC@I_h(7)$-C_{80}. The red arrows mark the split Sc_2UC cluster-cage-mode.

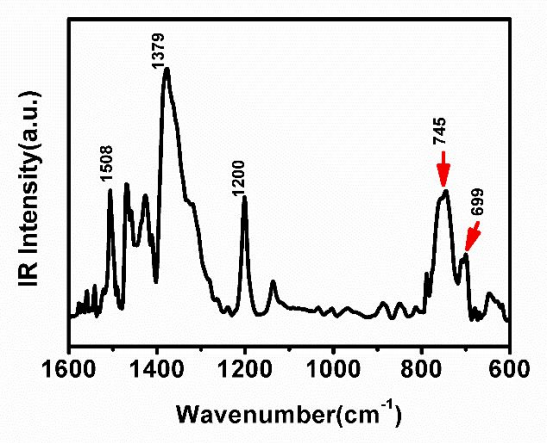

Figure 4. IR spectrum of $Sc_2UC@I_h(7)$-C_{80}. The red arrows mark the split asymmetric mode.

1600 cm^{-1} clearly resemble those of EMFs with the $I_h(7)$-C_{80} cage.[11] Among them, typical characteristics are the major overlaid bands around 1380 cm^{-1} and two minor peaks at 1130 and 1200 cm^{-1}, which could be assigned to the tangential cage modes of $I_h(7)$-C_{80}.[28,29] In the low-wavenumber range from 600 to 800 cm^{-1} , two pronounced peaks at 699 and 745 cm^{-1} can be observed, an asymmetric vibration splitting typical for the mixed cluster fullerenes, which have been detected for the anti-symmetric metal-N stretching mode in $Gd_xSc_{3-x}N@I_h(7)$-C_{80} (x = 1, 2) and $Sc_{3-x}Er_xN@I_h(7)$-C_{80} (x = 1, 2).[30,31] Thus the vibrational spectroscopic studies further confirm the mixed metallic Sc_2UC cluster configuration assigned by crystallographic analysis.

The redox properties of $Sc_2UC@I_h(7)$-C_{80} were investigated by means of cyclic voltammetry (CV), which exhibits three reduction peaks and one oxidation peak (see Figure 5), with only the 1st oxidation and the 1st reduction processes electrochemically reversible. This redox behavior is notably different from that of the $U_2C@I_h(7)$-C_{80}.[11] The first reduction potential of $Sc_2UC@I_h(7)$-C_{80} is -1.41 V, dramatically shifted from the -0.41V value observed for $U_2C@I_h(7)$-C_{80} (Table 1). Consequently, the electrochemical gap for $Sc_2UC@I_h(7)$-C_{80} is determined at 1.30 V, considerably larger than that of $U_2C@I_h(7)$-C_{80}. The different reversibility behavior and the potential differences of the two compounds suggest that the substitution of U atom by two Sc and the altered bonding motif in the encapsulated cluster exert a major impact on the frontier molecular orbitals (FMOs) and the resulting redox behavior of the actinide cluster fullerene.

On the other hand, although $Sc_2UC@I_h(7)$-C_{80} has similar bonding structures to that of the $Sc_2TiC@I_h(7)$-C_{80}, the first reduction and oxidation potentials of $Sc_2UC@I_h(7)$-C_{80} are dramatically more negative than those measured for $Sc_2TiC@I_h(7)$-C_{80} (Table 1).[21] The potential differences between the two also indicate that the substitution of Ti by U within the cluster has a major effect on the FMOs of the molecule.

In summary, a mixed actinide-lanthanide cluster fullerene, $Sc_2UC@I_h(7)$-C_{80}, was characterized by single crystal X-ray crystallography, UV–vis–NIR spectroscopy, Raman spectroscopy, Fourier transform infrared absorption spectroscopy and cyclic voltammetry. To the best of our

knowledge, Sc_2UC is the first mixed actinide-lanthanide cluster discovered in an isolated compound. Crystallographic analysis

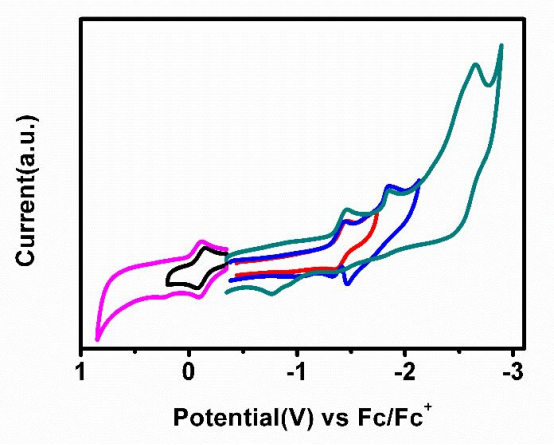

Figure 5. Cyclic voltammograms of $Sc_2UC@I_h(7)-C_{80}$ in $(n\text{-}Bu)_4NPF_6$/1,2-dichlorobenzene.

Table 1. Redox potentials (V vs. Fc/Fc^+) of $Sc_2UC@I_h(7)-C_{80}$ in comparison with $U_2C@I_h(7)-C_{80}$ and $Sc_2TiC@I_h(7)-C_{80}$.

compound	$E^{2+/+}$	$E^{+/0}$	$E^{0/-}$	$E^{-/2-}$	$E^{2-/3-}$	E_{gap}(V)
$Sc_2UC@I_h(7)-C_{80}$		-0.11[a]	-1.41[a]	-1.84[b]	-2.65[b]	1.30
$U_2C@I_h(7)-C_{80}$	+1.05[b]	+0.42[a]	-0.41[a]	-1.34[a]		0.83
$Sc_2TiC@I_h(7)-C_{80}$		+0.66[c]	-0.67[c]	-1.51[c]	-1.66[c]	1.33

[a] Half-wave potential(reversible redox process). [b] Peak potential (irreversible redox process). [c] DPV potential.

shows that the motion of Sc_2UC cluster is considerably hindered and the cluster is likely hopping inside the fullerene cage. In particular, a U-C bond distance of 2.01 Å observed for Sc_2UC cluster is the shortest U=C double bond confirmed by crystallography so far. The Raman and IR spectra further confirms the mixed actinide-lanthanide metallic cluster configuration. The electrochemical studies reveal the major impact of the substitution of U by two Sc on the FMOs of actinide cluster fullerenes. This study shows that the mixed actinide-lanthanide cluster fullerene possesses unique molecular and electronic structures which resemble neither its actinide nor lanthanide analogues, paving the way for future systematic study of these fascinating endohedral fullerenes.

Conflicts of interest

There are no conflicts to declare.

Notes and references

1 S. Stevenson, G. Rice, T. Glass, K. Harich, F. Cromer, M. R. Jordan, J. Craft, E. Hadju, R. Bible, M. M. Olmstead, K. Maitra, A. J. Fisher, A. L. Balch, H. C. Dorn, *Nature* 1999, **401**, 55-57.
2 A. A. Popov, S. Yang, L. Dunsch, *Chem. Rev.* 2013, **113**, 5989-6113.
3 S. Yang, T. Wei, F. Jin, *Chem. Soc. Rev.* 2017, **46**, 5005-5058.
4 I. Infante, L. Gagliardi, G. E. Scuseria, *J. Am. Chem. Soc.* 2008, **130**, 7459-7465.
5 X. Dai, Y. Meng, M. Xin, F. Wang, D. Fei, M. Jin, Z. Wang, R. Zhang, *Procedia Chem.* 2012, **7**, 528-533.
6 X. Wu, X. Lu, *J. Am. Chem. Soc.* 2007, **129**, 2171-2177.
7 A. K. Srivastava, S. K. Pandey, N. Misra, *Mater. Chem. Phys.* 2016, **177**, 437-441.
8 M. V. Ryzhkov, A. L. Ivanovskii, B. Delley, *Comput. Theor. Chem.* 2012, **985**, 46-52.
9 M. V. Ryzhkov, B. Delley, *Comput. Theor. Chem.* 2013, **1013**, 70-77.
10 D. Manna, T. K. Ghanty, *J. Phys. Chem. C* 2012, **116**, 25630-25641.
11 X. Zhang, W. Li, L. Feng, X. Chen, A. Hansen, S. Grimme, S. Fortier, D.-C. Sergentu, T. J. Duignan, J. Autschbach, S. Wang, Y. Wang, G. Velkos, A. A. Popov, N. Aghdassi, S. Duhm, X. Li, J. Li, L. Echegoyen, W. H. E. Schwarz, N. Chen, *Nat. Commun.* 2018, **9**, 2753.
12 C. Fuertes-Espinosa, A. Gómez-Torres, R. Morales-Martínez, A. Rodríguez-Fortea, C. García-Simón, F. Gándara, I. Imaz, J. Juanhuix, D. Maspoch, J. M. Poblet, L. Echegoyen, X. Ribas, *Angew. Chem. Int. Ed.* 2018, **57**, 11294-11299.
13 G. E. Sigmon, J. E. S. Szymanowski, K. P. Carter, C. L. Cahill, P. C. Burns, *Inorg. Chem.* 2016, **55**, 2682-2684.
14 N. P. Martin, C. Volkringer, N. Henry, S. Duval, D. Mara, R. Van Deun, T. Loiseau, *Cryst. Growth. Des.* 2018, **18**, 2165-2179.
15 K. E. Knope, D. T. de Lill, C. E. Rowland, P. M. Cantos, A. de Bettencourt-Dias, C. L. Cahill, *Inorg. Chem.* 2012, **51**, 201-206.
16 S.-P. Liu, M.-L. Chen, B.-C. Chang, K.-H. Lii, *Inorg. Chem.* 2013, **52**, 3990-3994.
17 W. Kratschmer, L. D. Lamb, K. Fostiropoulos, D. R. Huffman, *Nature* 1990, **347**, 354-358.
18 X. Zhang, Y. Wang, R. Morales-Martínez, J. Zhong, C. de Graaf, A. Rodríguez-Fortea, J. M. Poblet, L. Echegoyen, L. Feng, N. Chen, *J. Am. Chem. Soc.* 2018, **140**, 3907-3915.
19 A. L. Svitova, K. B. Ghiassi, C. Schlesier, K. Junghans, Y. Zhang, M. M. Olmstead, A. L. Balch, L. Dunsch, A. A. Popov, *Nat. Commun.* 2014, **5**, 3568.
20 F. Liu, F. Jin, S. Wang, A. A. Popov, S. Yang, *Inorg. Chim. Acta* 2017, **468**, 203-208.
21 K. Junghans, K. B. Ghiassi, N. A. Samoylova, Q. Deng, M. Rosenkranz, M. M. Olmstead, A. L. Balch, A. A. Popov, *Chem. – Eur. J.* 2016, **22**, 13098-13107.
22 T. Wei, S. Wang, X. Lu, Y. Tan, J. Huang, F. Liu, Q. Li, S. Xie, S. Yang, *J. Am. Chem. Soc.* 2016, **138**, 207-214.
23 S. Stevenson, C. B. Rose, J. S. Maslenikova, J. R. Villarreal, M. A. Mackey, B. Q. Mercado, K. Chen, M. M. Olmstead, A. L. Balch, *Inorg. Chem.* 2012, **51**, 13096-13102.
24 Y. Zhang, K. B. Ghiassi, Q. Deng, N. A. Samoylova, M. M. Olmstead, A. L. Balch, A. A. Popov, *Angew. Chem. Int. Ed.* 2015, **54**, 495-499.
25 Y.-X. Zhao, K. Yuan, M.-Y. Li, M. Ehara, X. Zhao, *Inorg. Chem.* 2019, **58**, 10769-10777.
26 W. Cai, R. Morales-Martínez, X. Zhang, D. Najera, E. L. Romero, A. Metta-Magaña, A. Rodríguez-Fortea, S. Fortier, N. Chen, J. M. Poblet, L. Echegoyen, *Chem. Sci.* 2017, **8**, 5282-5290.
27 W. Cai, C.-H. Chen, N. Chen, L. Echegoyen, *Acc. Chem. Res.* 2019, **52**, 1824-1833.
28 Krause, M.; Kuzmany, H.; Georgi, P.; Dunsch, L.; Vietze, K.; Seifert, G., *J. Chem. Phys. 2001*, **115**, 6596-6605
29 Yang, S.; Dunsch, L., *Eur. J. 2006,* **12**, 413–419
30 S. Yang, A. Popov, M. Kalbac, L. Dunsch, *Chem. – Eur. J.* 2008, **14**, 2084-2092.
31 L. Dunsch, M. Krause, J. Noack, P. Georgi, *J. Phys. Chem. Solids* 2004, **65**, 309-315.

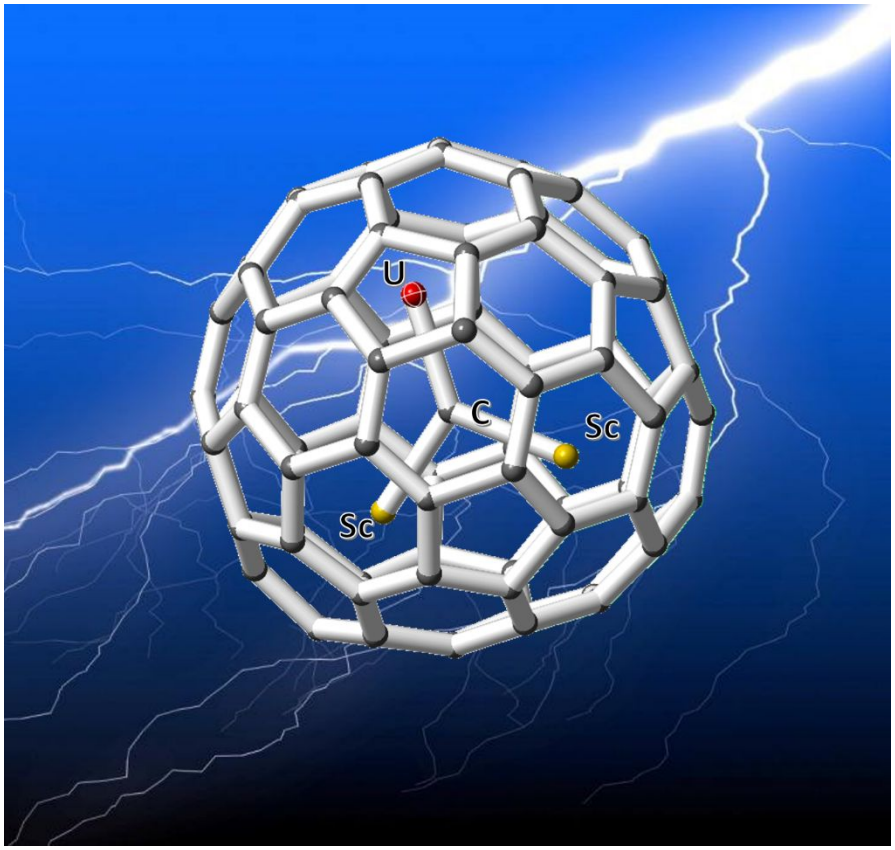

For the first time, crystallographic and spectroscopic analyses identified that a mixed actinide-lanthanide carbide cluster Sc_2UC, with a very short U=C bond, is stabilized inside an $I_h(7)$-C_{80} cage.